Available online at www.sciencedirect.com
SCIENCE DIRECT®
International Journal of Thermal Sciences 45 (2006) 635–642
International Journal of Thermal Sciences
www.elsevier.com/locate/ijts

# Boundary layer and stability analysis of natural convection in a porous cavity

Ali Bahloul

*Institut de Recherche Robet-Sauvé en Santé et Sécurité du Travail, 505, boul. de Maisonneuve Ouest, 14e étage, Montréal, PQ H3A 3C2, Canada*

Received 20 December 2004; received in revised form 2 August 2005; accepted 13 October 2005

Available online 17 November 2005

**Abstract**

Natural convection in a rectangular porous medium is studied analytically and numerically. The two vertical walls of the cavity are maintained at different temperature while the two horizontal ones are adiabatic. Governing parameters of the problem under study are the Rayleigh number, *Ra*, and the aspect ratio of the cavity, *A*. Numerical solutions of the full governing equations are obtained for a wide range of the governing parameters. For a large Rayleigh number, an approximative model of the boundary layer regime is obtained based on the numerical results. Simplified model for the stratification parameter, $\gamma$, have been obtained for high heating, $\gamma = 1.22A^{-0.47}Ra^{0.46}$. The thermal stratification coefficient, $\tau$, was shown to depend essentially on the aspect ratio of the enclosure, *A*, and becomes almost independent of the Rayleigh number, *Ra*, in the boundary layer regime, $\tau \approx 3/2A$. The linear stability theory of the parallel flow is employed to obtain the critical Rayleigh number (Hopf's bifurcation) for a tall cavity ($A \gg 1$). It is found that the flow is stable independent of the stratification coefficient, $\tau$.


*Keywords:* Natural convection; Instability; Porous media; Cavity; Boundary layer

## 1. Introduction

Natural convection has been a subject of intensive research in porous media, in view of its wide range of application in many engineering and technological areas. These include high performance insulation for building and cold storage, cooling of nuclear fuel in shipping flasks and water filled storage bays, insulation of high temperature gas cooled reactor vessels, burying of drums containing heat generating chemical in the earth, regenerative heat exchangers containing porous materials, etc.

Available studies on natural convection in confined porous media are concerned with the classical rectangular cavity, theses studies may be found in the recent books [1–7]. The possibility of obtaining parallel flow patterns has been reported many times in the literature. Bejan [8], for instance, described a parallel flow region in a thin, vertical, fluid saturated, porous cavity insulated on the sides and heated from the top by a constant flux. In the case of shallow cavities filled with a fluid, this time, the works of Cormack et al. [9,10] as well as Imberger [11] and Bejan and Tien [12] also mentioned the existence of parallel flow when different temperatures are imposed on the lateral sides of the cavity and the top and bottom are kept insulated. For a vertical enclosure heated from the sides by a constant flux, it was demonstrated that the dimensionless stratification coefficient (named dimensionless temperature gradient) depends only of Rayleigh number, *Ra*, when the cavity is very high ($A \gg 1$) [13–15]. While, it depends on the aspect ratio enclosure, *A*, for a fixed temperature difference, $\Delta T$, between the sides walls [16–19].

It is well known, both theoretically and experimentally, that the parallel flows mentioned above may become unstable at high Rayleigh numbers. In general, the critical value for the onset of the flow instability regime is strongly dependent on the boundary conditions imposed on the walls of the enclosure. Nield [20] showed that different instability regimes, in a shallow porous saturated layer submitted to an oblique temperature gradient, could be obtained by varying the vertical to lateral temperature gradient ratio. Kimura et al. [21] considered the stability problem for a porous medium in the same geometry as Nield, but this time for insulated vertical boundaries and a constant heat flux applied from below. They found a critical transition from the steady parallel base flow to an oscillatory instability regime. The linear stability of mixed convection in a heated vertical porous channel was investigated by Chen [22].

*E-mail address:* bahloul.ali@irsst.qc.ca (A. Bahloul).

1290-0729/$ – see front matter 
doi:10.1016/j.ijthermalsci.2005.10.003

**Nomenclature**

| | | | |
|---|---|---|---|
| $A$ | aspect ratio | $\beta_T$ | coefficient of thermal expansion ..... $K^{-1}$ |
| $D$ | derivative operator | $\gamma$ | stratification parameter |
| $C_p$ | specific heat at constant pressure ..... $J\,kg^{-1}\,K^{-1}$ | $\theta$ | base flow temperature profile |
| $g$ | gravity ..... $m\,s^{-2}$ | $\nu$ | kinematic viscosity ..... $m^2\,s^{-1}$ |
| $H'$ | height ..... m | $\mu$ | dynamic viscosity ..... $kg\,m^{-1}\,s^{-1}$ |
| $k$ | vertical wavenumber | $\rho$ | density ..... $kg\,m^{-3}$ |
| $k_T$ | thermal conductivity ..... $W\,m^{-1}\,K^{-1}$ | $\tau$ | thermal stratification coefficient |
| $K$ | permeability of the porous medium ..... $m^2$ | $\sigma$ | complex amplification rate |
| $L$ | operator | $\sigma_T$ | heat capacity ratio, $(\rho C_p)_p/(\rho C_p)_f$ |
| $L'$ | distance between the walls ..... m | $\psi$ | base flow stream function |
| $M$ | operator | $\omega$ | oscillation frequency |
| $N$ | number of grid points | | |
| $Ra$ | Rayleigh number, $= g\beta_T K \Delta T' L'/\alpha\nu$ | *Superscripts* | |
| $S$ | vertical temperature gradient | | |
| $t'$ | time ..... s | $'$ | dimensionless variable |
| $T'$ | temperature ..... K | *Subscripts* | |
| $\Delta T'$ | characteristic temperature differences, $= T'_1 - T'_2$ ..... K | $c$ | critical value |
| | | 0 | reference value |
| $u', v'$ | velocity components ..... $m\,s^{-1}$ | *Other symbols* | |
| $x', y'$ | coordinates ..... m | | |
| *Greek symbols* | | $\nabla$ | gradient |
| | | $\nabla^2$ | Laplacian |
| $\alpha$ | thermal diffusivity ..... $m^2\,s^{-1}$ | | |

It was demonstrated that the laminar flow could become unstable for a high Darcy number, but the critical Rayleigh number increases substantially for a low Darcy number.

For a fluid medium, Korpela et al. [23] determined that the instability in a vertical cavity with a fixed temperature difference on the sides is either of hydrodynamic or thermal origin depending on the Prandtl Number. They established that the critical modes are hydrodynamic and stationary if $Pr < 12.7$ and thermal and oscillatory if $Pr > 12.7$. The analysis was extended by Bergholz [18] to a wide range of Prandtl numbers and levels of stratification of the base flow. His work showed that transition from stationary to oscillatory modes occurs with increasing stratification at small Prandtl numbers, and from oscillatory to stationary at large Prandtl numbers. Suslov and Paolucci [24] also examined flow instability in a vertical cavity with a fixed temperature difference on the sides, but under non-Boussinesq conditions and without stratification of the base temperature field. They reported, assuming the transport properties of air for the active fluid, two modes of oscillatory instabilities: a shear-driven one for the smaller temperature differences and a buoyancy-driven one for the larger temperature differences.

In the present article, natural convection in a vertical porous cavity is considered. The article is organized as follows. In Section 2 the governing equations describing the problem are derived. An approximate solution for the basic state (laminar flow) is proposed in Section 3 for a fixed stratification parameter, $\gamma$. Section 4 describes the numerical method used to solve the problem. In the same section, the major results are discussed. A linear stability analysis of the basic state is investigated in Section 5, and a conclusion is presented in Section 6.

## 2. Problem statement

The physical model and coordinate system are shown in Fig. 1. The geometry of considered problem is a two-dimensional vertical enclosure of height $H'$ and width $L'$ filled with a saturated porous medium. The porous medium is considered to be uniform and in local thermal equilibrium with the fluid. The fluid is assumed to be incompressible and Newtonian.

A constant temperatures differences, $\Delta T' = T'_1 - T'_2$ is applied between the lateral boundaries, while the horizontal walls are adiabatic. The effect due to viscous dissipation and porous medium inertial are assumed to be negligible. The thermophysical parameters of the fluid are assumed to be constant, except for the density variation in the buoyancy term, which depends linearly on local temperature, i.e. Boussinesq approximation is supposed to be valid, where $\rho_0$ is the fluid density at temperature $T'_0$, and $\beta_T$ is the thermal expansion coefficient. The subscript "0" refers to conditions at the origin of the coordinate system.

$$\rho = \rho_0\left[1 - \beta_T(T' - T'_0)\right] \tag{1}$$

Based on Darcy's law, the governing equations for an isotropic porous medium are:

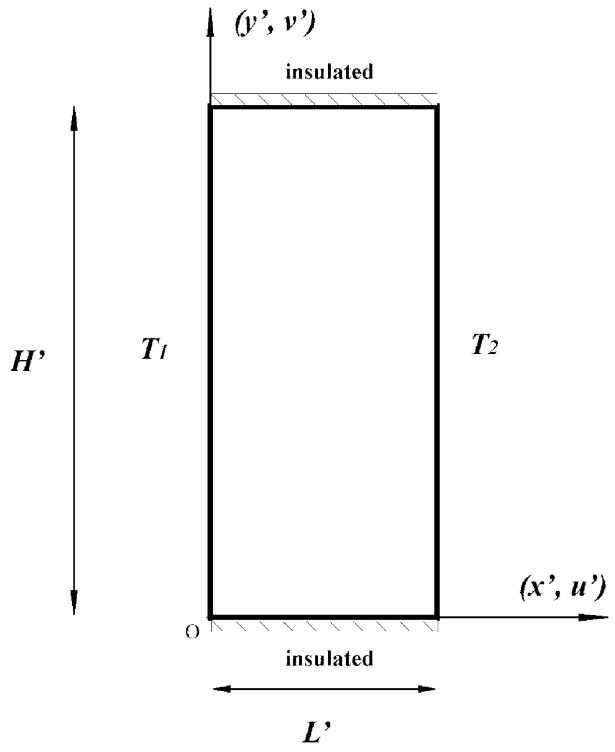


Fig. 1. Schematic diagram of the physical model and coordinate system.

$$\vec{\nabla}' \cdot \vec{V}' = 0 \tag{2}$$

$$\vec{\nabla}' p' + \rho \vec{g} + \frac{\mu}{K} \vec{V}' = 0 \tag{3}$$

$$\sigma_T \frac{\partial T}{\partial t} + (\vec{V}' \cdot \vec{\nabla}') T' = \alpha \nabla^2 T' \tag{4}$$

The boundary conditions, sketched in Fig. 1, are:

$$x' = 0, L'; \quad u' = 0, \ T'(0, y') = T_1', \ T'(L', y') = T_2' \tag{5}$$

$$y' = 0, H'; \quad v' = 0, \ \frac{\partial T'}{\partial y'} = 0 \tag{6}$$

These equations are based on the assumption that the viscous drag (Brinkman model) and inertia terms are neglected because their order of magnitudes are small compared to other terms for low Darcy numbers.

The following dimensionless variables are used

$$(x, y) = (x', y')/L', \qquad (u, v) = (u', v')L'/\alpha,$$
$$t = t'\alpha/L'^2\sigma_T$$
$$T = (T' - T_0')/\Delta T', \qquad \Delta T' = T_1' - T_2' \tag{7}$$

where $t'$ is the time, $\sigma_T$ is the ratio of composite material heat capacity to convective fluid heat capacity and $k_T$ and $\alpha = k_T/(\rho C_p)_f$ are the thermal conductivity and diffusivity, respectively, of the saturated porous medium.

In the following analysis, the stream function formulation is introduced in the mathematical model. In order to satisfy the continuity equation, the stream function $\Psi$ is defined such that $u = \partial\Psi/\partial y$ and $v = -\partial\Psi/\partial x$.

In terms of the above definitions, the dimensionless governing equations expressing conservation of momentum and energy are:

$$\nabla^2 \Psi = -Ra \frac{\partial T}{\partial x} \tag{8}$$

$$\frac{\partial T}{\partial t} + u \frac{\partial T}{\partial x} + v \frac{\partial T}{\partial y} = \nabla^2 T \tag{9}$$

The dimensionless boundaries, sketched in Fig. 1, are

$$x = 0, 1; \quad \Psi = 0, \ T(0, y) = \frac{1}{2}, \ T(1, y) = -\frac{1}{2} \tag{10}$$

$$y = 0, A; \quad \Psi = 0, \ \frac{\partial T}{\partial y} = 0 \tag{11}$$

The dimensionless parameters that characterize the problem are the aspect ratio of the enclosure $A = H'/L'$ and the thermal Rayleigh number $Ra = g\beta_T K \Delta T' L'/\alpha\nu$.

In the above definitions $K$ is the permeability of the porous medium, $g$ the acceleration due to gravity and $\mu$ the dynamic viscosity of the fluid.

## 3. Analytical solution

In order to obtain an approximative analytical solution, a temperature gradient, $S > 0$, is introduced in the vertical direction along each of the vertical walls (see for instance Bergholz [18]). The boundary conditions in horizontal direction used here are:

$$x = 0, 1; \quad \Psi = 0, \ T(0, \mathrm{y}) = \frac{1}{2} + \tau y, \ T(1, y) = -\frac{1}{2} + \tau y \tag{12}$$

where $\tau = SL'/\Delta T'$ is the dimensionless thermal stratification coefficient. A correlation of $\tau$ will be obtained by solving numerically the full equations (8) and (9) with the boundary conditions (10) and (11).

For sufficiently large values of the aspect ratio $A$, fully developed flow conditions are possible in the central part of the cavity, with streamlines nearly parallel with the y axis. In such a case, the parallel base flow can be described by a stream function of the form $\psi = \psi(x)$ only. The momentum equation (8) reduces to

$$D^2 \psi + Ra \frac{\partial T}{\partial x} = 0 \tag{13}$$

where $D = \frac{\mathrm{d}}{\mathrm{d}x}$ is derivative operator. With boundary conditions $\psi = 0$ for $x = 0$ or 1. Differentiating Eq. (13) with respect to $y$ shows that the temperature profile must have the form $T = \theta(x) + g(y)$. It follows from the temperature equation, Eq. (9), that $g(y)$ must be linear in $y$ in order to avoid trivial solutions for the stream function. The temperature field, up to an additive constant, is then given by

$$T = \theta(x) + \tau y \tag{14}$$

where $\tau > 0$ for stable stratification, while $\theta$ must satisfy the boundary conditions $\theta(0) = 1/2$ and $\theta(1) = -1/2$. The temperature equation may then be integrated once to get

$$\frac{\partial T}{\partial x} = D\theta = -\tau\psi + C_1 \tag{15}$$

where $C_1$ is a integration constant.

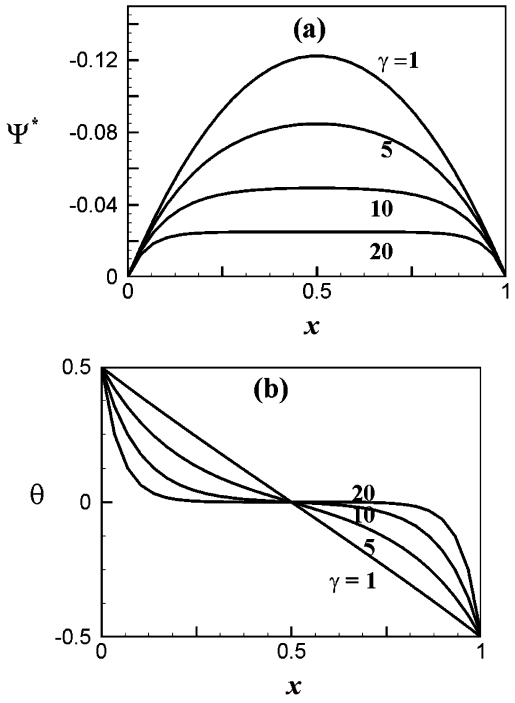


Fig. 2. (a) Stream function ($\Psi* = \Psi/Ra$) and (b) temperature profiles for different values of stratification parameter $\gamma$.

Eliminating now $T$ from Eq. (13) using Eqs. (14) and (15) leads to an equation in terms of $\Psi$ only

$$D^2\psi - \gamma^2\psi = -C_1 Ra \tag{16}$$

where

$$\gamma^2 = \tau Ra \tag{17}$$

The solution of set of Eqs. (16) and (17) satisfying the boundary conditions in the $x$-direction yields:

$$\psi(x) = \frac{Ra}{2\gamma \operatorname{sh}\frac{\gamma}{2}}\left[\operatorname{ch}\gamma\left(x-\frac{1}{2}\right) - \operatorname{ch}\frac{\gamma}{2}\right] \tag{18}$$

$$\theta(x) = -\frac{\operatorname{sh}\gamma(x-\frac{1}{2})}{2\operatorname{sh}\frac{\gamma}{2}} \tag{19}$$

From Eq. (18) it is found that the vertical velocity is given by:

$$v(x) = -Ra\frac{\operatorname{sh}\gamma(x-\frac{1}{2})}{2\operatorname{sh}\frac{\gamma}{2}} = Ra\,\theta(x) \tag{20}$$

The stream function and temperature profiles, $\Psi^*(x) = \Psi(x)/Ra$ and $\theta(x)$, are illustrated in Fig. 2 for different values of the stratification parameter, $\gamma$, ranging from 1 (pseudo conduction regime) to 20 (convection regime). A blocking effect of the vertical stratification in the temperature and stream function profiles occur at the center part of the cavity when $\gamma \geqslant \gamma_c \cdot \gamma_c$ is obtained from the analytical solution when the stream function and temperature profiles become flat at center of the cavity, it is found that $\gamma_c \approx 4.4$. In the limit $\gamma \to 0$ ($\tau \to 0$), $\Psi(x)$ and $\theta(x)$ approach the simple conduction profiles:

$$\psi(x) = \frac{Ra}{2}x(x-1), \qquad \theta(x) = \frac{1}{2} - x \tag{21}$$

In the limit, $\gamma \to \infty$ ($L' \to \infty$), the boundary layer solution is obtained for the flow adjacent to a single heated wall laterally bounding a stably stratified fluid:

$$\psi(x) = \frac{Ra}{2\gamma}\left(e^X - 1\right), \qquad \theta(x) = \frac{\delta e^X}{2} \tag{22}$$

where $X = \gamma(|x - \frac{1}{2}| - \frac{1}{2})$ and $\delta = 1$ for $x < \frac{1}{2}$ ($= -1$ for $x > \frac{1}{2}$).

## 4. Numerical solution

A finite-difference numerical solution technique based on integration over control volumes is used to solve the model equations with approximate boundary conditions. The hybrid scheme suggested by Patankar [25] was utilized. This scheme employs the powerlaw method only when the coefficient matrix becomes negative due to a large value of the velocity on the convection term. All other points are approximated by central differences. The application of the method to the solution of natural convection problems has been discussed in details in the past (see for instance [25]) and does not need to be repeated here.

In order to improve the resolution of dependent variables a non-uniform grid was used. The non-uniform grid has denser clustering near the wall boundaries. Grid independence of the results was established by employing different meshes, ranging in size from $60 \times 200$ to $80 \times 220$. The results indicated a maximum relative difference of about 1.2% in the value of the maximum stream function $\Psi_{\max}$. Additionally, the relative difference between both grids for the vertical velocity profile, at the center of the cavity, is less than 1%. Thus a $60 \times 200$ grid was used for all the results reported here.

To ensure convergence of the numerical algorithm the following criteria is applied to all dependent variables over the solution domain

$$\sum_i \sum_j \frac{|\phi_{i,j}^{n+1} - \phi_{i,j}^{n}|}{\sum_i \sum_j |\phi_{i,j}^{n+1}|} \leqslant 10^{-9} \tag{23}$$

where $\phi$ represents a dependent variable, the indexes $i$, $j$ indicate a grid point and the index $n$ the current iteration.

It is important to validate our calculation by trying to duplicate the recent results obtained by difference investigators [26–28]. Table 1 shows an excellent agreement between the present numerical results in terms of the average Nusselt number along the vertical walls of a square cavity ($A = 1$) and the numerical ones obtained in the past.

Typical numerical results are presented in Fig. 3 for $A = 2$ and different values of Rayleigh number, $Ra = 10, 200$ and 1000. On the graph streamlines and isotherms are presented in Figs. 3(a) and 3(b) respectively. If $Ra$ is small (pseudo conduction regime, $Ra = 10$), there is little variation of the fluid temperature with height, and heat is transferred between the vertical walls primarily by conduction. The flow pattern consists in a weak unicellular motion rotating in the clockwise direction along the cavity. However, as $Ra$ is increased, a stable vertical temperature gradient develops in the core of the

Table 1
Comparison of the average Nusselt number of the present investigation with existing results of in the case of the square cavity

| | Manole & Lage (1992) | Baytas (2000) | Nawaf & Pop (2003) | Present study | Analytical approximation |
|---|---|---|---|---|---|
| $Ra = 10^2$ | 3.118 | 3.160 | 3.002 | 3.110 | 5.074 |
| $Ra = 10^3$ | 13.637 | 14.060 | 13.726 | 13.715 | 14.632 |
| $Ra = 10^4$ | 48.117 | 48.330 | 43.953 | 47.132 | 42.202 |

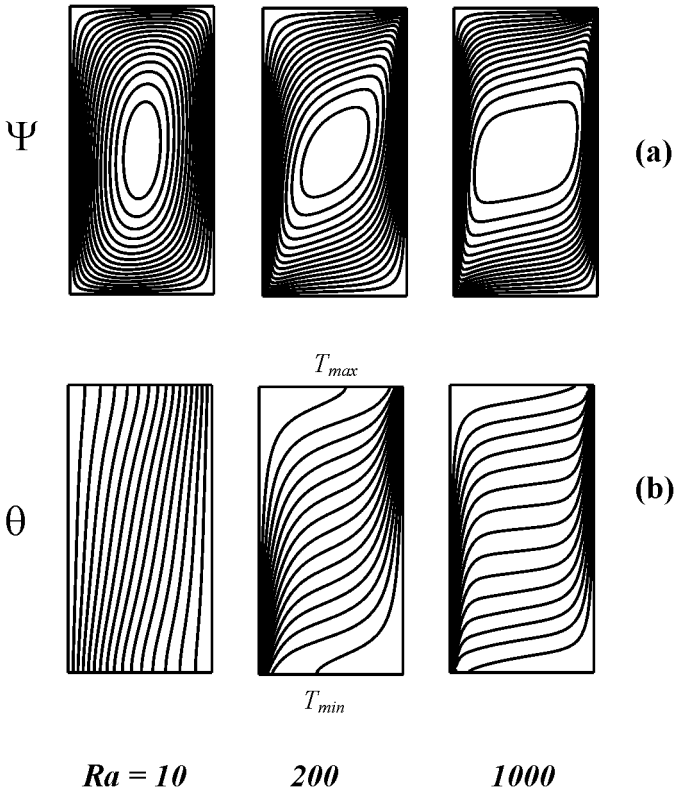


Fig. 3. Contour lines of (a) stream function and (b) temperature for $Ra = 10, 200$ and 1000 and $A = 2$.

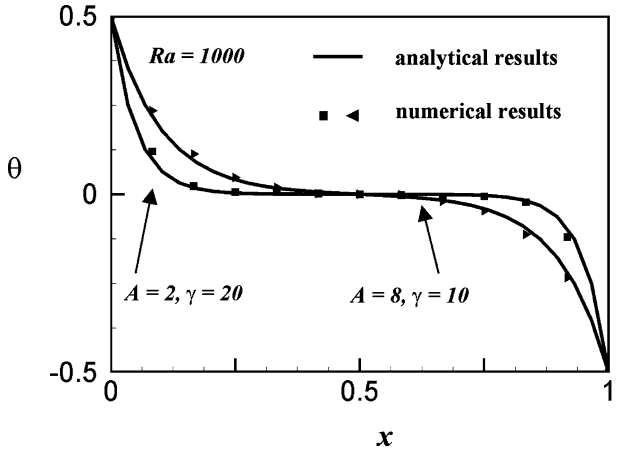


Fig. 4. Temperature profiles for the case $Ra = 1000$ and ($A = 2$ and $\gamma = 20$; $A = 8$ and $\gamma = 10$).

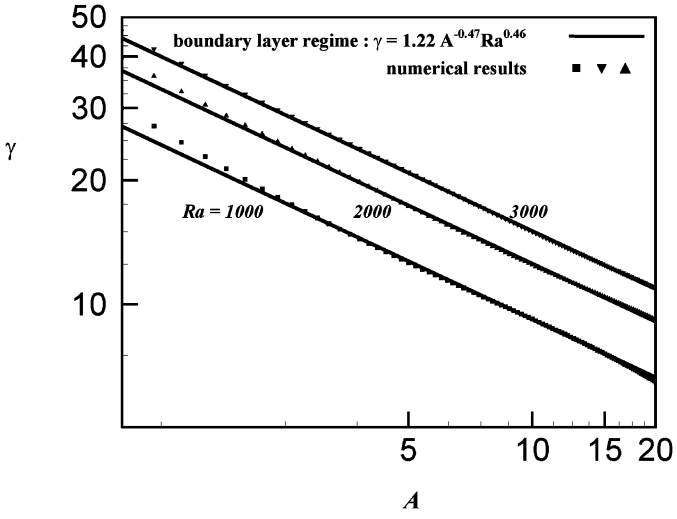


Fig. 5. Parameter of stratification, $\gamma$, as function of aspect ratio, $A$, for different values of $Ra$ ($Ra = 1000$, 2000 and 3000).

flow (transition regime, $Ra = 200$). The vertical thermal stratification introduce a vertical stratification of the density $\rho$. The heaviest part of the fluid is moved to the bottom of the cavity where the temperature is low, while the lightest one is in the top of the enclosure where the temperature is high. The fluid is now progressively stagnant in the core of the enclosure. Finally, if $Ra$ becomes sufficiently large (convection regime, $Ra = 1000$), the flow is confined to boundary layers at the side walls. A large portion of the fluid in the center of the cavity is now stagnant due to the blocking effect of the vertical stratification of the density field in this area and the flow circulation is restricted to thin boundary layers of almost constant thickness, along the vertical walls.

The stratification parameter, $\gamma$, is numerically calculated at the center of the cavity once convergence has been obtained. The temperature profile can be examined for the centerline ($y = A/2$) for a fixed Rayleigh number, $Ra = 1000$, and different values of aspect ratio, $A = 2$ and 8, as shown in Fig. 4. The numerical solution is displayed by depicted black dots in the graph and the values of the stratification parameter, $\gamma$, are 20 and 10 for $A = 2$ and 8 respectively. For this situation ($\gamma$ equal to 20 and 10) the analytical solution, displayed by solid lines, is seen to be in excellent agreement with the numerical solution of the full governing equations.

In the following paragraph, a correlation of the stratification parameter, $\gamma$, as a function of aspect ratio, $A$, and Rayleigh number, $Ra$, will be obtained based on the numerical results.

The effect of the aspect ratio, $A$, on the stratification parameter, $\gamma$, is exemplified in Fig. 5 for the cases of $Ra = 1000$, 2000, and 3000. For high value of $Ra$ considered here, the heat transfer reaches the boundary layer regime. For this situation, the stratification parameter linearly depend on the aspect ratio in

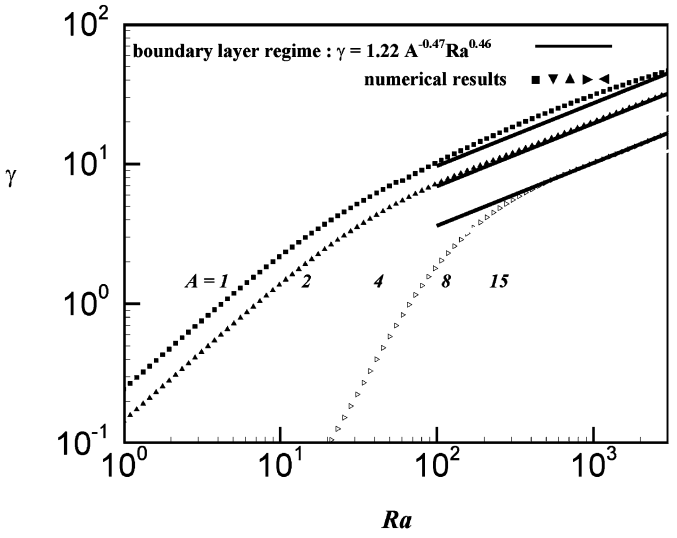


Fig. 6. Parameter of stratification, $\gamma$, as function of Rayleigh number, $Ra$, for different values of $A$ ($A = 1, 2, 4, 8$ and 15).

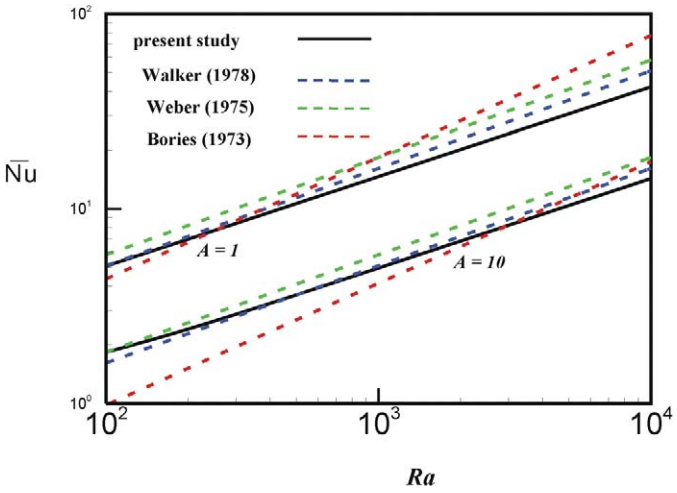


Fig. 7. Maximal growth rate, $\sigma$, as function of Rayleigh number, $Ra$, and vertical wavenumber, $k$, for different values of stratification parameter, $\gamma$.

logarithmic scale used in the graph. Based on the numerical results, a simplified model of $\gamma$ is obtained for the boundary layer regime. The parameter of stratification, $\gamma$, depends on $A$ as: $\gamma = CA^{-0.47}$, where $C$ is constant that varies with $Ra$. The graph indicates that for $A \geqslant 2$, this model, displayed by solid lines, is seen to be in excellent agreement with the numerical results.

The variation of $\gamma$ with $Ra$ is illustrated in Fig. 6 for the cases of $A = 1, 2, 4, 8$ and 15. The graph indicates that when $Ra$ is small enough, convection is weak and the stratification parameter, $\gamma$, is very small ($\gamma \to 0$), such that heat transfer is ruled by pure diffusion (pseudo conduction regime). Upon increasing the Rayleigh number, convection is promoted, a stable vertical temperature gradient is developed (transition regime) and $\gamma$ is increased. Finally, a boundary layer regime is reached when the Rayleigh number becomes sufficiently large (convection regime). Here again, the graph shows that the stratification parameter, $\gamma$, varies as power law of $Ra$ in logarithmic scales. A final simplified model of $\gamma$ as function of the control parameters of the problem under study is obtained and we have:

$$\gamma = 1.22A^{-0.47}Ra^{0.46} \tag{24}$$

Fig. 6 shows that this correlation is in an excellent agreement with the numerical results when $A \geqslant 2$ and $Ra \geqslant 500$.

From the approximative analytical solution developed in this study and the present correlation of stratification parameter, $\gamma$, an approximative correlation of the Nusselt average number, $\overline{Nu}$, is easily obtained. Based of the results Eq. (24), A correlation of $\overline{Nu}$ is deducted from Eq. (19):

$$\overline{Nu} = \gamma_0 \coth(\gamma_0) \tag{25}$$

where $\gamma_0 = \frac{\gamma}{2} = 0.61A^{-0.47}Ra^{0.46}$.

For $\gamma_0 \gg 1$, Eq. (25) is reduced to:

$$\overline{Nu} = 0.61A^{-0.47}Ra^{0.46} \tag{26}$$

Table 1 shows a quite good agreement between the analytical approximation and the numerical ones of the Nusselt number average along the vertical walls of a square cavity ($A = 1$) even where the Rayleigh number is low. The margin of errors between numerical and analytical results is due to the small aspect ratio ($A = 1$) and the boundary effects.

In the past [29–32], analytical works have included numerical solutions, boundary layer solutions, integral analysis and series solutions. Based on theses studies, various correlations of $\overline{Nu}$ have been presented, and these cover a wide range of Rayleigh numbers and aspect ratios. It is worthwhile to considered theses correlations of $\overline{Nu}$ and the one presented here.

In the boundary layer regime, Walker and Homsy [29] have concluded a correlation of the average Nusselt number as:

$$\overline{Nu} = (0.51 \pm 0.01)Ra^{0.5}A^{-0.5} \tag{27}$$

and Weber [30] have obtained

$$\overline{Nu} = 0.58Ra^{0.5}A^{-0.5} \tag{28}$$

The numerical result of Bories and Combarnous's study [31] is

$$\overline{Nu} = 0.245Ra^{0.625}A^{-0.647} \tag{29}$$

In Fig. 7, the present results have compared with the above existing numerical results for two values of aspect ratio $A = 1$ and 10. As can be seen, the present correlation of Nusselt number average is in excellent agreement with most of the results in the past for both low and high Rayleigh numbers.

Whereas, the experimental work of Sokie et al. [32] shows that

$$\overline{Nu} = 0.627Ra^{0.473}A^{-0.472} \tag{30}$$

As we can see, the above experimental correlation of $\overline{Nu}$ is closer to the one developed in this work than the numerical ones developed in the past.

The pertinent parameter of the problem under study is the dimensionless vertical temperature gradient 'temperature stratification coefficient', $\tau$. A correlation of $\tau$ is deducted from Eq. (21) and the temperature stratification coefficient, $\tau$, is given by:

$$\tau = \gamma^2/Ra = 1.49A^{-0.94}Ra^{-0.04} \approx \frac{3}{2A} \tag{31}$$

For high aspect ratio and high heating, the dimensionless temperature gradient parameter, $\tau$, should be proportional to $\Delta T/A$, where $\Delta T = 1$ is the dimensionless characteristic temperature difference. As expected, Eq. (28) shows that $\tau$ depends essentially on $1/A$, and becomes almost independent of the Rayleigh number in the boundary layer regime when a Newman thermal boundary conditions are applied across the vertical walls. However, for Dirichlet thermal boundary conditions, $\Delta T$ varies with *Ra* and the dimensionless temperature gradient parameter highly depends of Rayleigh number (see for instance [15]).

## 5. Linear stability analysis

Let small amplitude perturbations of the temperature and stream function field components of the form

$$\widetilde{F} = \widetilde{F}(x)\exp[st + iky] \tag{32}$$

be added to the base flow Eqs. (16)–(18), where $\widetilde{F}$ is a complex quantity, $k$ is the real vertical wavenumber, and $s = \sigma + \mathrm{i}\omega$ is the complex amplification rate (the wavenumber can be taken as real since the vertical walls are supposed to be of infinite extent in the $y$ direction). Substitution of the sum of the base flow and perturbation variables, into the set of governing equations Eqs. (6)–(7), followed by linearization to first order in small quantities yields the system of equations

$$\begin{aligned}&\left(D^2 - k^2\right)\widetilde{\Psi} + Ra\,D\widetilde{T} = 0\\ &\left[D^2 - k^2 - ikV(x)\right]\widetilde{T} + \left[\tau D - ikD\theta(x)\right]\widetilde{\Psi} = s\widetilde{T}\end{aligned} \tag{33}$$

in which $D$ is equal to $\mathrm{d}/\mathrm{d}x$.

This set of equations, together with the boundary conditions $\widetilde{\Psi} = \widetilde{T} = 0$ at $x = 0$; 1, defines an eigenvalue problem in $s$ for a given set of parameter values *Ra*, $\gamma$ and $k$.

Solution of Eq. (33) above can be achieved in several ways. One of the most straightforward is to discretize the equations by finite-differences. Fourth and second-order central difference schemes are employed throughout; the eigenvalues of the resulting discrete system are found using a standard IMSL subroutine such as EIGENC or QZ. The eigenvalue problem is solved iteratively, holding $\gamma$, $k$ constant and seeking by Newton's method the value of *Ra* for which the maximal growth rate $\sigma$ cancels. Repeating the procedure for different wavenumbers $k$ determines a marginal stability curve for the given value of $\gamma$. The minimum value of *Ra* over all the stability curves corresponds to the critical Rayleigh number $Ra_c(q, \gamma)$.

Using finite-difference schemes to solve the eigenvalue problem requires a larger number of computational points $N$ to obtain accurate results than, say, Chebyshev or spectral methods. The computational time needed to achieve convergence remains quite reasonable however. It is instructive to validate our approach by trying to duplicate the results obtained by Bergholz [18] with Galerkin's method for fluid medium. Table 2 shows excellent agreement between the values of the critical Grashof number $Gr_c = Ra_c/Pr$ calculated by Bergholz using from 24 to 30 eigenfunctions and by us using $N = 100$ computational points. Table 1 shows also the comparison between the present numerical results and the experimental ones obtained by difference investigators [18,19] and [33,34].

Table 3 shows a comparison between the results predicted by the above numerical procedure and those reported in the past by Mamou et al. [35] and Kimura et al. [21] for the case of thermal convection within an infinite layer heated from bellow by a constant flux. The critical Rayleigh number, the critical wave length and the corresponding frequency for Hopf bifurcation obtained here are seen to be in excellent agreement with the values reported in the past.

The linear stability theory of the parallel flow is employed for the present study to obtain the critical Rayleigh number for a tall cavity ($A \gg 1$). It is found that the maximal growth rate $\sigma$ is always negative for all values of the Rayleigh number, *Ra*, stratification coefficient, $\tau$, and the vertical wavenumber, $k$ (Fig. 8). Consequently, the parallel flow state remains stable independently of stratification parameter, $\gamma$, for the porous media case.

## 6. Conclusion

Analytical and numerical results are reported for natural convection of a fluid in a vertical porous cavity. A uniform temperature difference is applied across the vertical walls while the horizontal ones are adiabatic. The linear stability theory has been used to predict the marginal state of instability via stationary convection or oscillatory motions. The main finding of the present investigation are:

(1) With the thermal boundary conditions considered in this investigation it has been demonstrated numerically that the flow is almost parallel and the isotherms are stratified in the core of the cavity provided that aspect ratio $A$ is large enough. This point is the basis of the approximate analytical model developed here. The resulting analytical model

Table 2
Comparison of results of the present investigation with existing results of Bergholz and available experiment data in the case of the fluid medium in term of $Gr_c$

| Experiment | | | | | | Theoretical | |
|---|---|---|---|---|---|---|---|
| *Pr* | $\gamma$ | *A* | Elder (1965) | Hart (1971) | Vest & Arpaci (1969) | Bergholz (1978) | Present $N = 100$ |
| 0.71 | 2.21 | 33.33 | n/a | n/a | $8.7 \times 10^3$ | $8.92 \times 10^3$ | $8.931 \times 10^3$ |
| 6.7 | 4.32 | 37.04 | n/a | $1.5 \times 10^4$ | n/a | $1.53 \times 10^4$ | $1.526 \times 10^4$ |
| 6.7 | 4.73 | 25 | n/a | $1.94 \times 10^4$ | n/a | $1.20 \times 10^4$ | $1.193 \times 10^4$ |
| 900 | 6.89 | 20 | n/a | n/a | $4.11 \times 10^2$ | $4.00 \times 10^2$ | $3.981 \times 10^2$ |
| 1000 | 6.91 | 19 | $3.3 \times 10^2$ | n/a | n/a | $3.47 \times 10^2$ | $3.468 \times 10^2$ |

Table 3
Comparison of results of the present investigation with existing results of in the case of the porous media in term of $Ra_c$

| | Kimura et al. (1995) | Mamou et al. (1999) | Present study |
|---|---|---|---|
| $Ra_c$ | 506.07 | 506.07 | 506.02 |
| $k_c$ | 4.825 | 4.825 | 4.825 |
| $f_c$ | 22.11 | 22.11 | 22.11 |

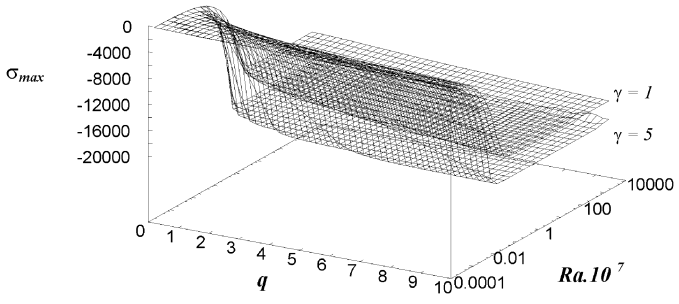


Fig. 8.

requires a determination of the stratification parameter by using the numerical results.

(2) Useful approximate expressions have been obtained by the numerical results to describe the boundary layer regime. Simplified model for the stratification parameter have been obtained for high heating. The thermal stratification coefficient was shown to depend essentially on the aspect ratio of the enclosure, and becomes almost independent of the Rayleigh number in the boundary layer regime.

(3) The linear stability theory of the parallel flow is employed to obtain the critical Rayleigh number for a tall cavity ($A \gg 1$). It is found that the flow is stable independent of the stratification coefficient.

## References

[1] D.-A. Nield, A. Bejan, Convection in Porous Media, second ed., Springer, New York, 1999.
[2] K. Vafai, Handbook of Porous Media, Marcel Dekker, New York, 2000.
[3] A. Bejan, A.-D. Kraus, Heat Transfer Handbook, Wiley, New York, 2003.
[4] D.-B. Ingham, I. Pop, Transport Phenomena in Porous Media, Pergamon, Oxford, 1998, vol. I, 2002; vol. II, 2005.
[5] I. Pop, D.-B. Ingham, Convective Heat Transfer: Mathematical and Computational Modelling of Viscous Fluids and Porous Media, Pergamon, Oxford, 2001.
[6] D.-B. Ingham, A. Bejan, E. Mamut, I. Pop, Emerging Technologies and Techniques in Porous Media, Kluwer Academic, Dordrecht, 2004.
[7] A. Bejan, I. Dincer, S. Lorente, A.-F. Miguel, A.-H. Reis, Porous and Complex Flow Structures in Modern Technologies, Springer, New York, 2004.
[8] A. Bejan, The boundary layer regime in a porous layer with uniform heat flux from the side, Int. J. Heat Mass Transfer 26 (1983) 1339–1346.
[9] D.-E. Cormack, J. Leal, L.-G. Imberger, Natural convection in a shallow cavity with differentially heated end walls, part 1: Asymptotic theory, J. Fluid Mech. 65 (1974) 209–229.
[10] D.-E. Cormack, L.-G. Leal, J.H. Seinfeld, Natural convection in a shallow cavity with differentially heated end walls, part 2: Numerical solutions, J. Fluid Mech. 65 (1974) 231–246.
[11] J. Imberger, Natural convection in a shallow cavity with differentially heated end walls, part 3: Experimental results, J. Fluid Mech. 65 (1974) 247–260.
[12] A. Bejan, C.L. Tien, Laminar natural convection heat transfer in a horizontal cavity with different end temperatures, J. Heat Transfer 100 (1978) 641–647.
[13] O. Trevisan, A. Bejan, Mass and heat transfer by natural convection in a vertical slot filled with porous medium, Int. J. Heat Mass Transfer 29 (1986) 403–415.
[14] F. Alavyoon, On natural convection in vertical porous enclosures due to prescribed fluxes of heat and mass at the vertical boundaries, Int. J. Heat Mass Transfer 36 (1993) 2479–2498.
[15] N. Boutana, A. Bahloul, P. Vasseur, F. Joly, Soret and double diffusive convection in a porous cavity, J. Porous Media 7 (1) (2004) 41–57.
[16] G.-K. Batchelor, Heat transfer by free convection across a closed cavity between vertical boundaries at different temperatures, Quart. Appl. Math. 12 (1954) 209–233.
[17] A.-E. Gill, The boundary layer regime for convection in a rectangular cavity, J. Fluid Mech. 26 (1966) 515–536.
[18] R.-F. Bergholz, Instability of steady natural convection in a vertical fluid layer, J. Fluid Mech. 84 (1978) 743–768.
[19] J.-W. Elder, Laminar free convection in a vertical slot, J. Fluid Mech. 23 (1965) 77–98.
[20] D.-A. Nield, Convection in a porous medium with inclined temperature gradient, Int. J. Heat Mass Transfer 34 (1991) 87–92.
[21] S. Kimura, M. Vynnycky, F. Alavyoon, Unicellular natural circulation in a shallow horizontal porous layer heated from below by a constant flux, J. Fluid Mech. 294 (1995) 231–257.
[22] Y.-C. Chen, Non-Darcy flow stability of mixed convection in a vertical channel filled with a porous medium, Int. J. Heat Mass Transfer 47 (2004) 1257–1266.
[23] S.-A. Korpela, D. Gözüm, C.-B. Baxi, On the stability of the conduction regime of natural convection in a vertical slot, Int. J. Heat Mass Transfer 16 (1973) 1683–1690.
[24] S.-A. Suslov, S. Paolucci, Stability of natural convection flow in a tall vertical enclosure under non-Boussinesq conditions, Int. J. Heat Mass Transfer 38 (1995) 2143–2157.
[25] S.-V. Patankar, Numerical Heat Transfer and Fluid Flow, Hemisphere, Washington, DC, 1980.
[26] D.-M. Manole, J.-L. Lage, Numerical benchmark results for natural convection in a porous medium cavity, in: Heat and Mass Transfer in Porous Media, ASME Conference, in: HTD, vol. 216, 1992, pp. 55–60.
[27] A.-C. Baytas, Entropy generation for natural convection in an inclined porous cavity, Int. J. Heat Mass Transfer 43 (2000) 2089–2099.
[28] N.-H. Nawaf, I. Pop, Transient free convection in a square cavity filled with a porous medium, Int. J. Heat Mass Transfer 47 (2004) 1917–1924.
[29] K.-L. Walker, G.-M. Homsy, Convection in a porous cavity, J. Fluid Mech. 97 (1978) 449–474.
[30] J.-E. Weber, The boundary layer regime for convection in a vertical porous layer, Int. J. Heat Mass Transfer 20 (1975) 569–573.
[31] S.-A. Bories, M.-A. Combarnous, Natural convection in a sloping porous layer, J. Fluid Mech. 57 (1973) 63–93.
[32] N. Seki, A. Fukusako, H. Inaba, Heat transfer in a confined rectangular cavity packed with a porous media, Int. J. Heat Mass Transfer 21 (1978) 985–989.
[33] C.-M. Vest, V.-S. Arpaci, Stability of natural convection in a vertical slot, J. Fluid Mech. 36 (1969) 1–15.
[34] J.-E. Hart, Stability of the flow in a differentially heated inclined box, J. Fluid Mech. 47 (1971) 547–576.
[35] M. Mamou, P. Vasseur, Thermosolutal bifurcation phenomena in porous enclosures subject to vertical temperature and concentration gradients, J. Fluid Mech. 395 (1999) 61–87.